Toughness Enhancement of Polyamide 6 Modified with Different Types of Rubber: The Influence of Internal Rubber Cavitation

G. BURGISI, M. PATERNOSTER, N. PEDUTO, A. SARACENO

Sniaricerche ScpA, Via Pomarico, 75010 Pisticci Scalo (MT), Italy

Received 17 March 1997; accepted 22 April 1997

ABSTRACT: The toughening enhancement of Polyamide 6 blended with different types of functionalized elastomers was studied. Morphological analysis by scanning electron microscopy (SEM) were performed on undeformed samples in order to determine particle–size distribution. Yet more SEM examination of the damage zone ahead of notch tip in uniaxial tensile test provided insight into the failure mechanisms. The best impact strength was achieved with the PA6/EPDM-*g*-MA (terpolymer ethylene–propylene–diene monomer grafted with Maleic Anhydride) blend, unlike ULDPE-*g*-MA (ultra-low-density polyethylene grafted with maleic anhydride), which possesses the poorest toughening efficiency even though opposite results would be expected from particle–size evaluation. The higher cavitation resistance of EPDM compared to ULDPE observed during low strain rate tensile test plays a crucial role in understanding the best performances of its blends. © 1997 John Wiley & Sons, Inc. J Appl Polym Sci **66:** 777–787, 1997

Key words: nylon 6–rubber blend; impact enhancement; fracture toughness; particle size; rubber cavitation

INTRODUCTION

Polyamides are defined as pseudoductile polymers, such as polycarbonate (PC) and polyvinylchloride (PVC) because their high energy for craze initiation compared to so-called brittle matrices as polystyrene (PS) and poly(styrene-acrylonitrile) (SAN). Pseudoductile matrices deform under a uniaxial tensile stress state mainly by shear yielding, whereas crazing is the deformation mechanisms of brittle matrices.

Nevertheless, polyamides become brittle in the presence of molding flaws, environmental abuse, poor design, or, more generally, in the presence of a stress concentrator that limits their industrial application.

However, it is well known that the addition of an elastomeric phase properly functionalized with a coupling agent greatly enhance their toughness, so polyamide-based multiphase systems have recently achieved great commercial success.

Furthermore, the presence of rubber particles in the polyamide matrix induces a sharp brittle ductile transition temperature (BDTT).

An extensive collection of literature attempts to explain the mechanisms by which the toughness of polyamides enhances by incorporating rubber particles.

Margolina and Wu[1] developed a correlation between impact and interparticle distance showing that smaller particles behave as better toughening agents; furthermore, according to Borggreve et al.,[2] the BDTT also decreases with smaller dispersed particle size. However, at very

Correspondence to: N. Peduto, Nyltech Italia, Via I Maggio 80, 20020 Ceriano Laghetto (MI), Italy.

Journal of Applied Polymer Science, Vol. 66, 777–787 (1997)
 CCC 0021-8995/97/040777-11

low particle size, i.e., below 0.2 μm for polyamides, the impact strength decreases sharply approaching the value of the unmodified matrix.[3] This behavior had been found by Sultan and McGarry[4] also in rubber-modified epoxy.

Borggreve et al.[5] had demonstrated that the mechanical properties of the impact modifier have a decisive influence on toughening polyamides, whereas the concentration of coupling agent does not have a great influence.

In rubber-modified polyamide 6,[2,5–7] and also in rubber-modified PC,[8–10] PVC,[11,12] and epoxy,[13] submitted to a triaxial stress state, cavitation of the rubber particles happens. This phenomenon is responsible for the macroscopic effect of stress whitening, which clearly appears.

Lazzeri and Bucknall[14,15] consider that cavitation happens at a level of volumetric strain lower than yield stress promoting shear yielding within dilatational bands.

Li et al.[16] have observed that for rubber-modified epoxy, fracture toughness does not improve if cavitation is suppressed.

Moreover, the cavitation resistance of the rubber particles is thought to be an important parameter to enhance toughness.[10,13]

In this study, the different mechanical performances of Polyamide 6 modified with four different types of rubber were investigated. To understand which parameters are the most important in enhancing the impact strength, rubber particle size and cavitation behavior of impact modifiers under a triaxial stress state were examined. Furthermore, a correlation between the cavitation resistance of rubbers inside the matrix and the critical stress intensity factor (K_{IC}) was given.

EXPERIMENTAL PART

Materials

Polyamide 6 (relative viscosity of 2.7), commercialized as ASN 27 S supplied by NYLTECH ITALIA, was used as the matrix phase. Four different types of rubber functionalized with maleic anydryde (MA), were used as the dispersed phase. More specifically, the rubbers used were as following: a terpolymer etylene–propylene–diene monomer (EPDM), a copolymer ethylene–propylene (EP), triblock copolymers having styrene endblocks and an hydrogenated butadiene midblock resembling an ethylene–butene copolymer (SEBS), and an ultra-low-density polyethylene (ULDPE). The rubbers are grafted with the same amount of coupling agent ($\cong$0.6%). Furthermore, it is worth pointing out that the rubbers possess a melt viscosity significantly different.

The rubbers can react with the Polyamide 6 matrix to form graft copolymers. The Polyamide 6 matrix were dried at 110°C under vacuum overnight before use. The concentration of the rubbers in blends were fixed at 25% by weight.

Blend Preparation

Blends were prepared by melt extrusion in a corotating twin screw extruder (Werner & Pfleiderer ZSK 25) setting the processing conditions (in terms of feed rate and screw speed) so as to assure the same specific energy parameter (*Ls* measured in KW$*$h/Kg) for all the blends. *Ls* is defined as the ratio of power provided by the extruder to the compound to the extruder throughoutput. The value of *Ls* was around 0.2 KW$*$h/Kg.

The extruder barrel has ten zones. The temperatures set up along the barrel were 245°C for zone 1; 250°C for zones 2 and 3; 260°C for zones 4 and 5; 270°C for zones 6 and 7, 260°C for zones 8 and 9, and 275°C for the die. The resultant strand was quenched in water and pelletized. After drying, pellets were molded in bar specimen using an ENGEL injection molding machine.

Charpy Impact Testing

Three point bend specimens (SENB) were prepared in order to evaluate the critical stress intensity factor (K_{IC}), which is a test designed to characterise the toughness of plastics. The dimension of the specimens were 3.2 mm in thickness and 12.3 mm in width, respectively. In order to assure a brittle fracture, specimens were frozen at a temperature of 35°C for half an hour before impact. The specimens were prenotched at different notched lengths in the range $0.45 < a/w < 0.55$. The K_{IC} value was calculated using the formula

$$K_{IC} = YP/BW^{1/2} \quad (1)$$

where P is the load at fracture, B is the thickness, W is the width, and Y is the compliance calibration factor.

Mechanical Testing

Tensile yield strength of the four samples was measured on ASTM D638 specimens using an INSTRON 6500 machine.

Table I Notched Izod Impact Strength Values at the Temperatures Ranging from 23 to −40°C for PA6 25% Rubber Blends

	Notched Izod Strength (J/m)				
Materials	23°C	0°C	−20°C	−30°C	−40°C
PA6-EPDM-*g*-MA	1130	1100	1100	700	155
PA6-EP-*g*-MA	920	850	800	565	150
PA6-SEBS-*g*-MA	1000	800	600	200	130
PA6-ULDPE-*g*-MA	950	500	415	150	125

SEM Analyses

A scanning electron microscope was used to measure the rubber particle size and particle size distribution and to evidence rubber phase cavitation.

The injection-molded specimens were broken cryogenically in liquid nitrogen, and the elastomeric modifier was extracted from the surface by etching with boiling decahydronaftalene. After sputter coating with a thin film of gold, the specimens were examined in a JEOL JSM 6300 scanning electron microscope. Particle analysis was then performed on SEM micrographs by using the analySIS commercial image analysis package.

To evidence the rubber phase cavitation, double notched specimens of each blend have been subjected to uniaxial tensile stress as far as a stress value of 40 and 70% of the yield stress has been reached, then cryogenically broken after one hour of immersion in liquid nitrogen. The specimens were then examined by SEM.

Rheological Measurements

The melt viscosity of the neat matrices and their blends were explored at the process temperature as a function of shear rate using a capillary extrusion rheometer. The Rabinowitsch corrections were made.

RESULTS AND DISCUSSION

Fracture Toughness Evaluation

In this investigation, the fracture toughness was evaluated by both Izod impact testing and critical stress intensity factor (K_{IC}) measurement. Impact testing is a popular and easy way to evaluate rubber-toughened polymers. The Izod impact test is very useful for comparing the toughening efficiencies of different impact modifiers.

Table I shows the Izod impact strength of all the blends at the temperatures ranging from 23 to −40°C. The thickness of the examined specimens was 3.18 mm. The data presented show the highest values at all temperatures for PA 6/EPDM-*g*-MA and together with PA 6/EP-*g*-MA possesses also the lowest value of BDTT, which is around −30°C for these two blends. The blend with SEBS-*g*-MA has a quite high value of impact until −20°C, comparable with the EP-*g*-MA blend; however, it possesses a higher BDTT than both EPDM-*g*-MA and EP-*g*-MA. Finally, the toughening efficiency of ULDPE-*g*-MA is the worst among the four elastomers examined, showing either the lowest impact value at all temperatures or the highest BDTT.

The K_{IC} is known as fracture toughness and it is a material property; the calculated K_{IC} values for the blends give a comparison of toughness efficiency because they represent, physically, the value that the stress intensity factor (KI) has to achieve for crack propagation.

K_{IC} was evaluated on injection molding specimens by means of an instrumented Charpy pendulum at temperature of −35°C. At this temperature, the impact behavior of all blends became brittle. The values of K_{IC} are reported in Table II. It was found that the PA 6/EPDM-*g*-MA blend gives the highest value of K_{IC}, whereas the PA 6/ULDPE-*g*-MA is the worst one, actually confirming what found in Izod impact testing.

Table II K_{IC} Values for PA6 25% Rubber Blends

Materials	K_{IC} at −35°C (Mpa*m$^{1/2}$)
PA6-EPDM-*g*-MA	3.76
PA6-EP-*g*-MA	3.37
PA6-SEBS-*g*-MA	3.10
PA6-ULDPE-*g*-MA	3.04

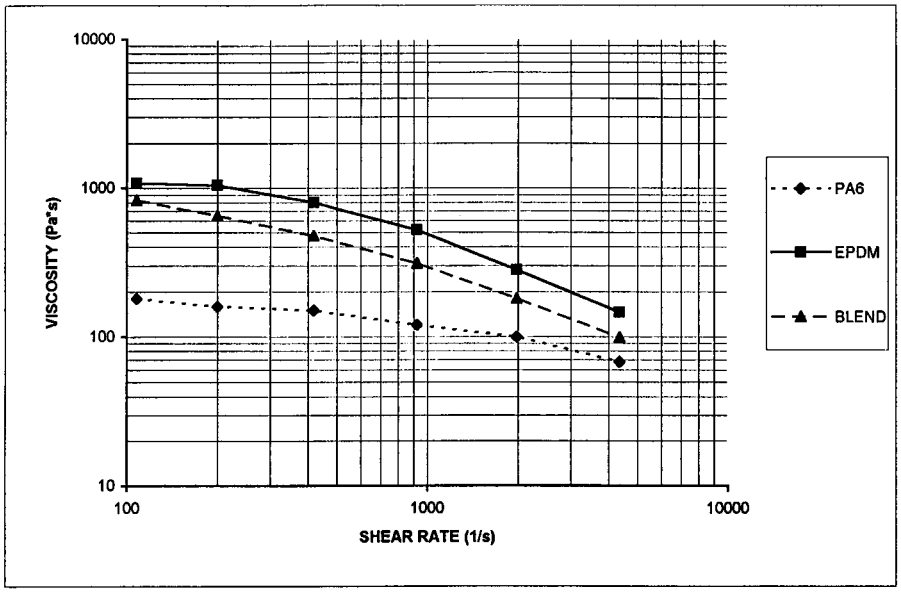

(a)

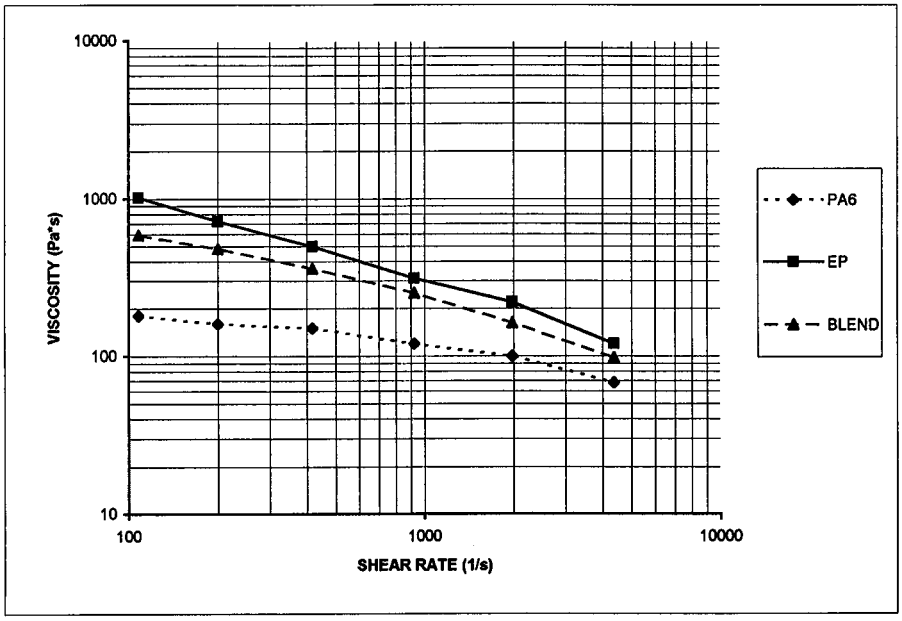

(b)

Figure 1 (a) Rheological curves of PA6, EPDM-*g*-MA, and their blend at 280°C. (b) Rheological curves of PA6, EP-*g*-MA, and their blend at 280°C.

Blend's Rheology and Rubber Particle Size Distribution

The importance of rheology in this context is well known; in fact, the rheological properties of the individual components strongly influence the product during processing.

Figures 1(a) and (b) and 2(a) and (b) show the melt viscosity of Polyamide 6 rubbers and blends calculated at 280°C, which was the temperature of the melt into the extruder. From the processing conditions, the shear rate of the process is located around 300 1/s.

It is evident from the plots that the EPDM-*g*-

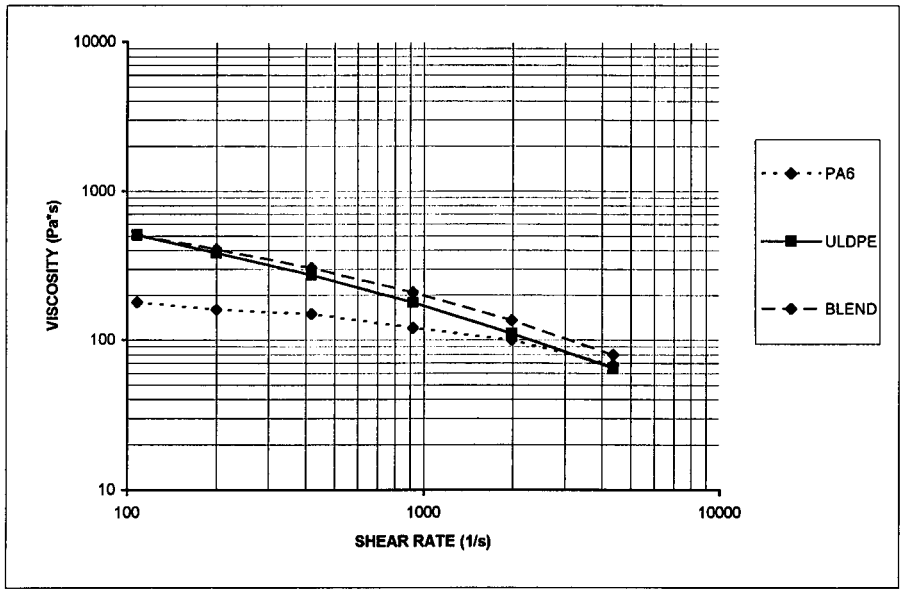

(a)

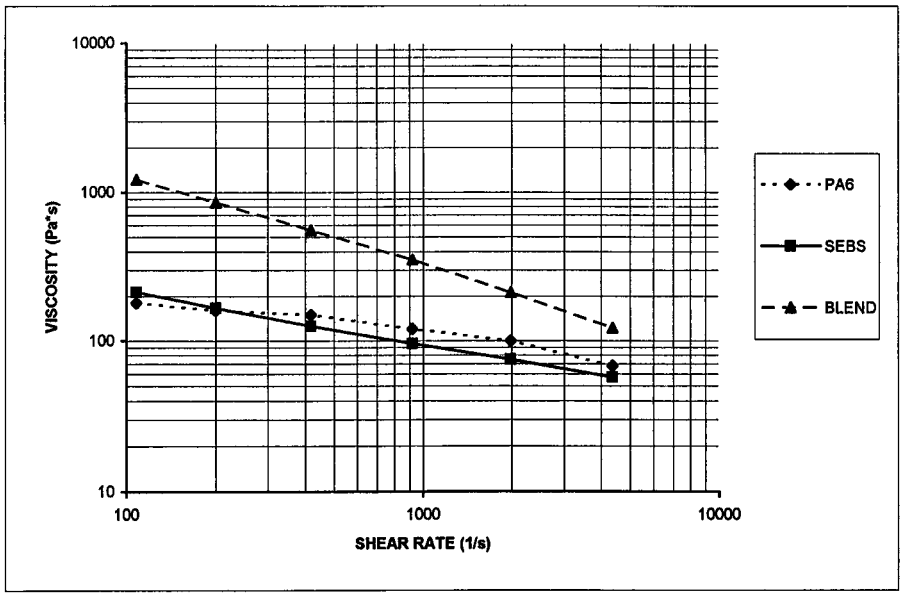

(b)

Figure 2 (a) Rheological curves of PA6, ULDPE-*g*-MA, and their blend at 280°C. (b) Rheological curves of PA6, SEBS-*g*-MA, and their blend at 280°C.

MA and EP-*g*-MA rubbers are much more viscous than the matrix in all ranges of shear rate. Unlike them, ULDPE-*g*-MA possesses a slighter higher viscosity with respect to PA 6, whereas SEBS-*g*-MA is very similar to the matrix. All the rubbers increase the viscosity of Polyamide 6 as expected due to the chemical reaction that takes place between the components. In the case of blends with higher viscosity rubbers, the blend curves are located more or less between the components due to the very high viscosity of the modifiers; on the contrary, for blends with ULDPE-*g*-MA and SEBS-*g*-MA, the blend curves are located above both of components.

Particle size distribution of the undeformed specimens was obtained examining the fractured

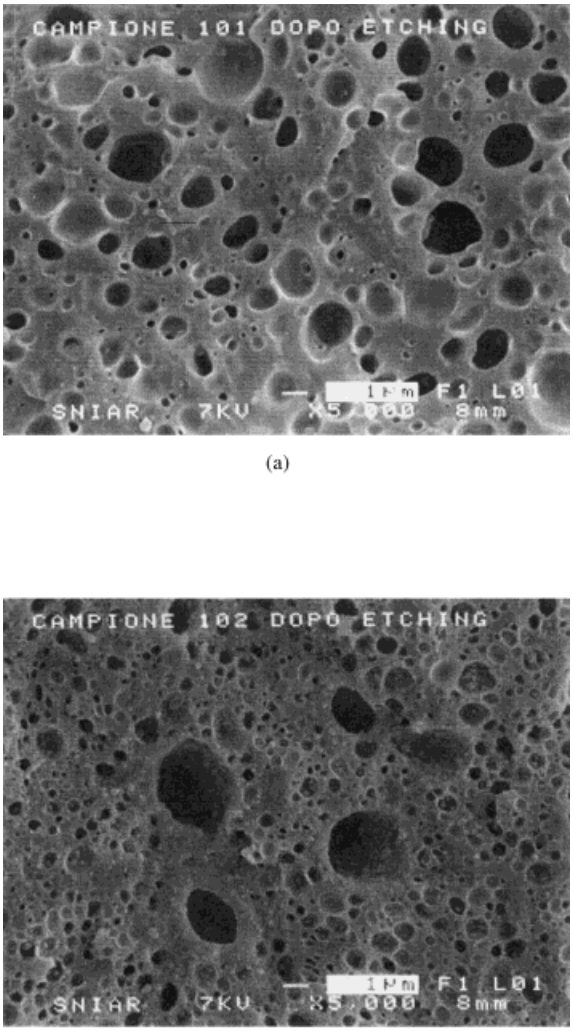

(a)

(b)

Figure 3 (a) SEM micrograph of undeformed PA6/EPDM-*g*-MA after etching in decahydronaphtalene. (b) SEM micrograph of undeformed PA6/ULDPE-*g*-MA after etching in decahydronaphtalene.

surfaces by SEM of bar specimens cryogenically broken perpendicular to the injection direction. Figure 3(a) and (b) report SEM micrographs of PA6/EPDM-*g*-MA and PA6/ULDPE-*g*-MA, respectively.

Approximately 500 particles selected randomly were counted using an image analyser. Figure 4(a) and (b) report the particle–size distribution of PA6/EPDM-*g*-MA and PA6/ULDPE-*g*-MA, respectively. It should be noted for all these blends that there is the presence of a small amount of big particles (with diameter greater than 2 μm). This observation can be explained by the fact that the both particles dispersion and particle size distribution of dispersed functionalized rubber are sensitive to the processing conditions as reported in a previous article.[17] The blends investigated in the present work have not been obtained at the optimum value of processing conditions, which have been chosen in order to assure a minimum residence time so as to avoid any degradation of the components. On the other hand, our aim was basically to evaluate the influence of the type of rubber, keeping every other parameter constant.

The figures illustrate that the blend with ULDPE-*g*-MA has the narrowest distribution and

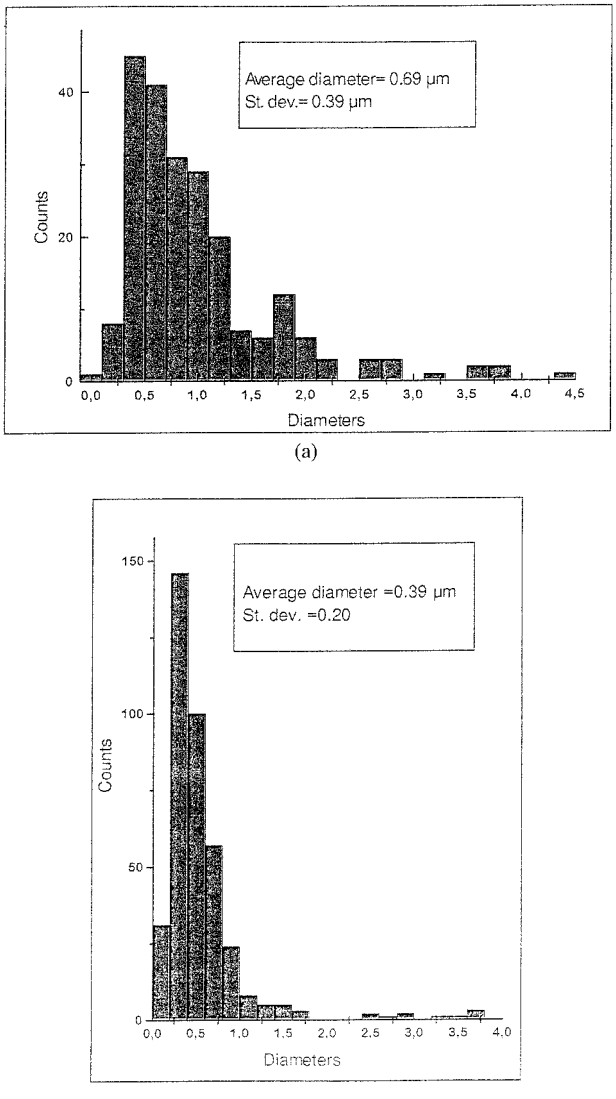

(a)

(b)

Figure 4 (a) Rubber particle size distribution in PA6/EPDM-*g*-MA. (b) Rubber particle size distribution in PA6/ULDPE-*g*-MA.

Table III A Comparison of K_{IC} Values and Average Particle Diameters for PA6 25% EPDM-*g*-MA and ULDPE-*g*-MA

Materials	K_{IC} (Mpa*m$^{1/2}$)	Average Particle Diameter (μm)
PA6-EPDM-*g*-MA	3.76	0.69
PA6-ULDPE-*g*-MA	3.04	0.39

the one most skewed towards small particle sizes. Table III reports the value of average particle size for the four blends compared with the correspondent values of K_{IC}. The reason for such morphological features underlies the rheological behavior of the two individual components. The breaking up of the particles is governed by the viscous forces and interfacial forces, and the Weber number gives the ratio between them. Wu[18] reports the master curve of the critical Weber number versus the viscosity ratio for various blends. For all the blends, we can consider that the interfacial tension between PA and rubbers is very similar and very low (0.25 mJ m^{-1}), in all cases due to the fact that the presence of coupling agent confers polarity to the rubbers. As a consequence, the Weber number depends exclusively on the viscous force; and from the master curve, its value appears to be the lowest, at the viscosity ratio equal to 1. This means that a decrease of the difference between the matrice's viscosity results in a decrease of the dispersed particle's size. These conclusions explain well what appears from the SEM micrographs.

The comparison between particle size distribution and mechanical performances reported in Table III clearly indicates that the difference in effectiveness of different types of elastomer cannot be understood by investigating only the morphological parameters; indeed, the impact enhancement was downright adversely affected by the morphology. In other words, the rubber particle size is an influential factor, as generally accepted; but its influence may vary from one system to another, and it would not be decisive. As a consequence, the investigation of deformation mechanisms had to be performed.

Relationship of Cavitation Condition and Impact

The investigation of the cavitation behavior of rubbers inside the matrix under triaxial stress state has been made in order to better understand the real reason of the impact enhancement. The voiding phenomena are measured under the low strain rate test, whereas the impact test involves high strain rate condition. However, the stress field around the rubber particles is triaxial anyway in both tests, so to correlate the cavitation phenomena checked under tensile test with the impact values is not physically incorrect.

A criterion for rubber cavitation was given[14,15,19]; the phenomenon happens when the elastic energy stored in the rubber particle under the applied stress is greater than the energy required to create a new surface by cavitation. The necessary condition for the enhancement of the impact is that rubber particles must cavitate at a level of stress lower than that for the crazing of the matrix in order to relieve triaxiality and prevent brittle fracture.

When rubber particle cavitate, if two voids are close enough, the matrix in between yields locally. If all the voids are close enough, the yield will propagate throughout the matrix, conferring ductility to it. This happens when the distance between voids (matrix ligament) and, thus between rubber particles, is lower than a critical value; and this morphological condition is achieved, decreasing rubber diameters and improving dispersion of particles. However, there is a lower limit of particles diameter (0.2 μm for polyamides[3]), after which cavitation does not happen anymore; and the impact behavior drops off, achieving the typical value of the unmodified matrix. It is generally accepted that the less particles, the higher the cavitation resistance.

On the other hand, cavitation of the particles rubber is dependent not only on rubber particles size but also on the elastic and molecular properties of the rubber. In fact, the criterion for rubber cavitation involves the rubber bulk modulus (Gent's criterion) and the energy per unit area associated with chain scission.

From the micrographs taken at various locations in the stress whitening zone [Fig. 5(a) and (b)] at 40% of yield stress, the cavitation mechanism seems to be concentrated in the first 300 μm far from the notch tip and tends to be more extended (700 μm) for specimens stressed at 70% of yields stress. The micrographs both referred to the sample with ULDPE-*g*-MA, but the same behavior was observed in the others. It should be noticed that the void diameter is larger for blends with EPDM-*g*-MA according to the larger particles diameter.

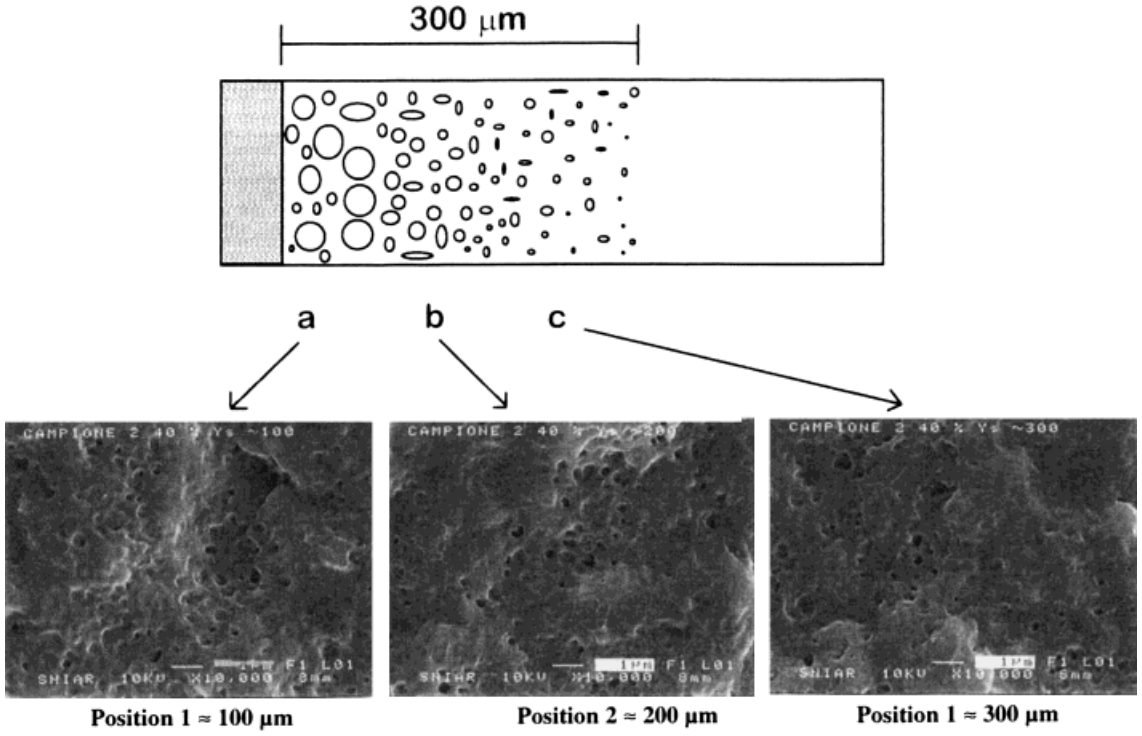

(a)

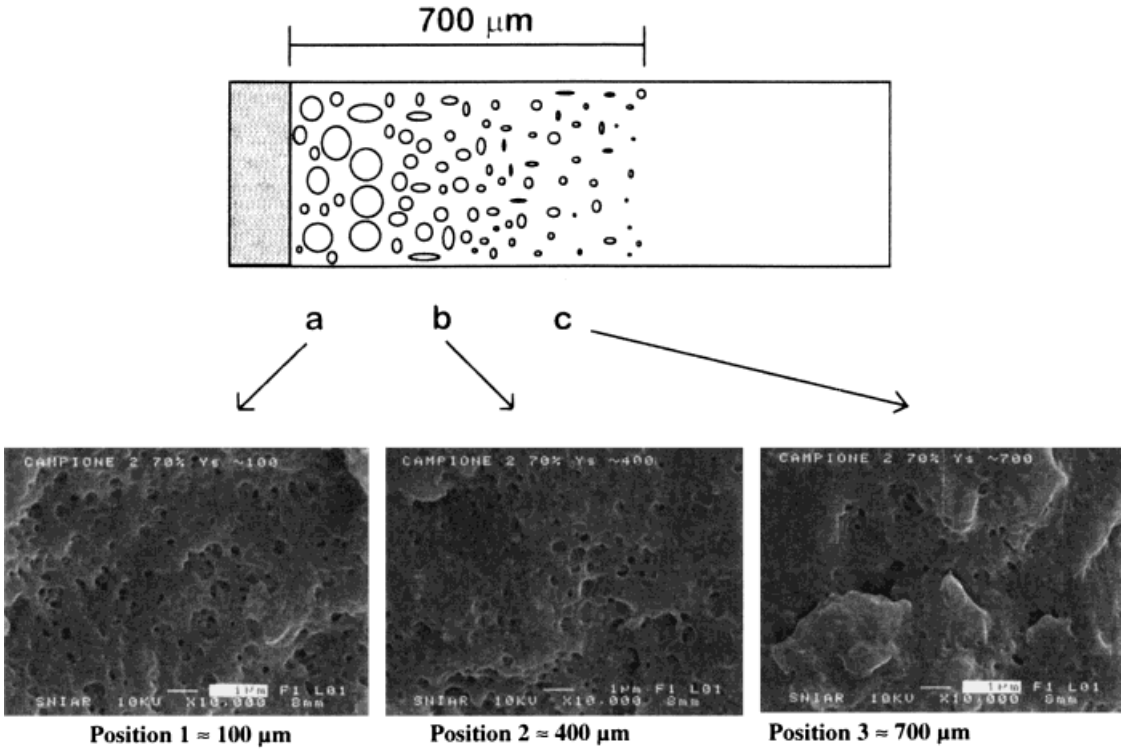

(b)

Figure 5 (a) SEM micrographs at different locations in the stress-whitened zone in PA6/ULDPE-*g*-MA tensile stressed as far as 40% Ys. (b) SEM micrographs at different locations in the stress-whitened zone in PA6/ULDPE-*g*-MA tensile stressed as far as 70% Ys.

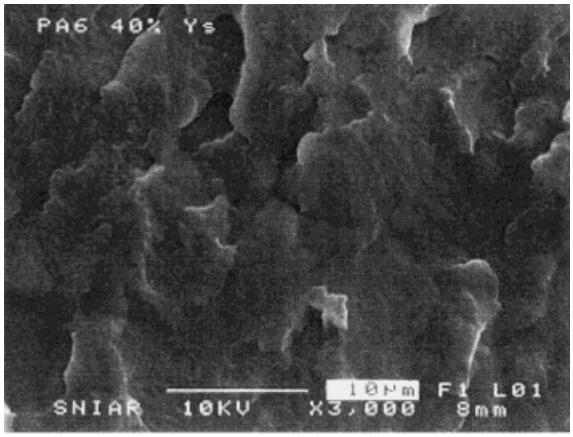

(a)

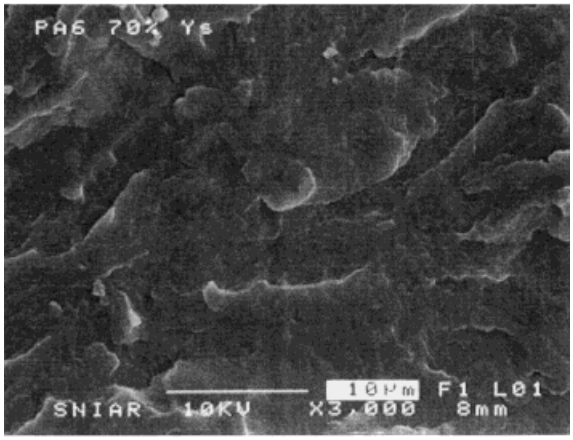

(b)

Figure 6 (a) SEM micrograph of PA6 matrix tensile stressed as far as 40% Ys. (b) SEM micrograph of PA6 matrix tensile stressed as far as 70% Ys.

Moreover, in order to be sure that cavitation phenomena interest the rubber phase and not the matrix, the same tensile test was made on neat PA 6. Figure 6(a) and (b) clearly demonstrates that any voiding formation is totally absent.

From the micrographs reported in Figures 7(a) and (b) and 8(a) and (b), we have calculated the number fraction of cavitated particles (F) at both levels of strain for blends with the highest (EPDM-*g*-MA) and lowest (ULDPE-*g*-MA) mechanical performances using an image analyser. The fraction is the ratio of the number of cavitated particles per unit area counted on the stressed samples to the total number of particles counted in the correspondent undeformed etched specimens per the same unit area. The results are shown in Table IV.

From Table IV, it appears that for Polyamide 6 modified by EPDM-*g*-MA, the fraction of cavitated particles is lower than the blend modified by ULDPE-*g*-MA; as a consequence, we can conclude that EPDM has a higher cavitation resistance, notwithstanding the larger particles diameter. The higher cavitation resistance increases the energy absorbed by cavitation, leading to better mechanical performances, accordingly to what was postulated for PC[10] and PVC[13] blends.

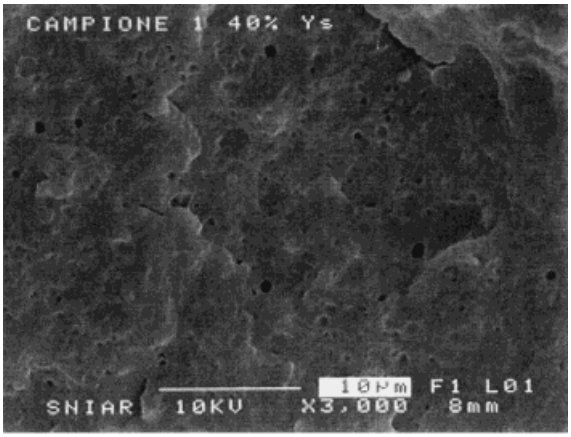

(a)

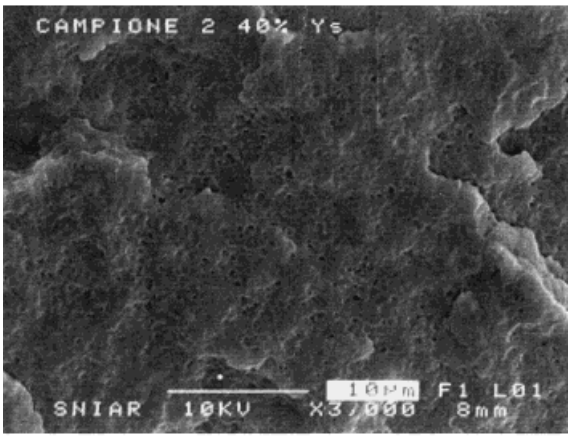

(b)

Figure 7 (a) SEM micrograph of the damage zone ahead of the notch tip in PA6/EPDM-*g*-MA tensile stressed as far as 40% Ys. (b) SEM micrograph of the damage zone ahead of the notch tip in PA6/ULDPE-*g*-MA tensile stressed as far as 40% Ys.

CONCLUSIONS

The analysis performed on the damage zone ahead of a sharp notch of rubber-modified Polyamide 6 deformed during slow tensile loading helped to compare quantitatively the cavitation behavior among four different types of rubber.

The study led to the following conclusions.

1. The toughening efficiency of the four examined different types of rubber functionalized with maleic anhydryde is ranked as

EPDM-*g*-MA > EP-*g*-MA > SEBS-*g*-MA > ULDPE-*g*-MA.

2. ULDPE, which is the worst among the modifiers investigated, exhibits the narrowest particle size distribution, which is also more skewed towards small particle sizes. It appears that the impact resistance increases with an increase in the average particles diameter.
3. The analysis of the damage zone in slow tensile loading reveals that at the same level of strain, EPDM has a higher cavitation resistance than ULDPE. The higher impact performances given by EPDM rubber compared to ULDPE is therefore attributed to the higher cavitation resistance of EPDM.

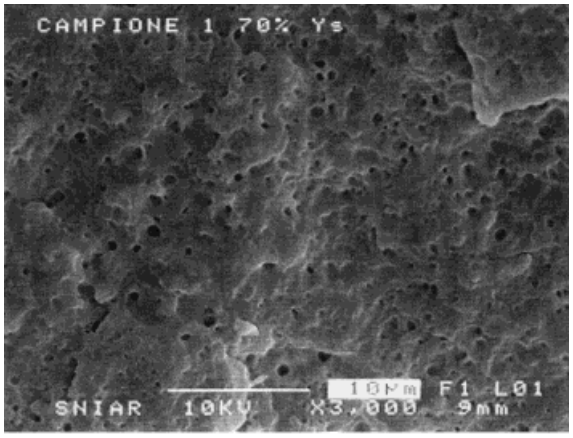

(a)

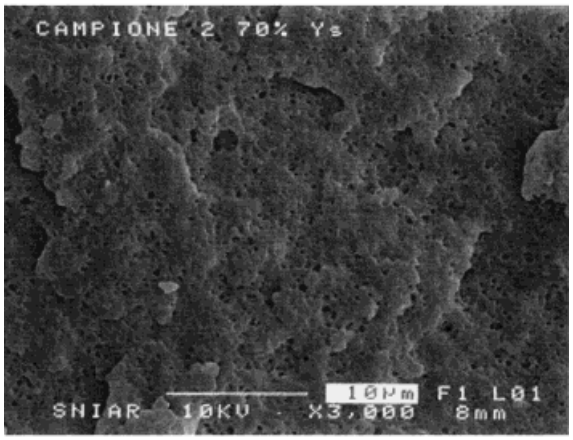

(b)

Figure 8 (a) SEM micrograph of the damage zone ahead of the notch tip in PA6/EPDM-*g*-MA tensile stressed as far as 70% Ys. (b) SEM micrograph of the damage zone ahead of the notch tip in PA6/ULDPE-*g*-MA tensile stressed as far as 70% Ys.

Table IV Fraction of Cavitated Particles (*F*) Calculated at Both Levels of Yield Stress (40 and 70%) for PA6 25% EPDM-*g*-MA and PA6 25% ULDPE-*g*-MA

Materials	*F* at 40% Ys (%)	*F* at 70% Ys (%)
PA6-EPDM-*g*-MA	6	23
PA6-ULDPE-*g*-MA	15	41

REFERENCES

1. A. Margolina and S. Wu, *Polymer,* **29,** 2170 (1988).
2. R. J. M. Borggreve, R. J. Gaymans, J. Schuijer, and J. F. Ingen Housz, *Polymer,* **28,** 1489 (1987).
3. A. J. Oostenbrink, K. Dijkstra, S. Wiegersma, A. van der Wal, and R. J. Gaymans, paper presented at PRI International Conference on Deformation, Yield and Fracture of Polymers, Cambridge, April, 1990.
4. J. N. Sultan and F. J. McGarry, *Polym. Eng. Sci.,* **13,** 29 (1973).
5. R. J. M. Borggreve and R. J. Gaymans, *Polymer,* **30,** 63 (1989).
6. F. Speroni, E. Castoldi, P. Fabbri and T. Casiraghi, *J. Mat. Sci.,* **24,** 2165 (1989).
7. R. J. M. Borggreve, R. J. Gaymans, and J. Schuijer, *Polymer,* **30,** 71 (1989).
8. D. S. Parker, H. J. Sue, J. Huang, and A. F. Yee, *Polymer,* **31,** 2267 (1990).
9. C. Cheng, N. Peduto, A. Hiltner, E. Baer, P. R.

Soskey, and S. G. Mylonakis, *J. Appl. Polym. Sci.,* **55,** 1691 (1994).
10. C. Cheng, A. Hiltner, E. Baer, P. R. Soskey, and S. G. Mylonakis, *J. Appl. Polym. Sci.,* **53,** 1691 (1995).
11. A. Tse, E. Shin, A. Hiltner, E. Baer, and R. Laakso, *J. Mat. Sci.,* **26,** 2823 (1991).
12. D. Dompas, G. Groeninckx, M. Isogawa, T. Hasegawa, and M. Kadokura, *Polymer,* **35,** 4750 (1994).
13. R. A. Pearson and A. F. Yee, *J. Mater. Sci.,* **26,** 3828 (1991).
14. A. Lazzeri and C. B. Bucknall, *J. Mater. Sci.,* **28,** 6799, 1993.
15. A. Lazzeri and C. B. Bucknall, *Polymer,* **36,** 2895, 1995.
16. D. Li, A. F. Yee, I. W. Chen, S. C. Chang, and K. Takahashi, *J. Mater. Sci.,* **29,** 2205, 1994.
17. M. Paternoster, A. Saraceno, and C. Armanni, paper presented at the 7th International Conference on Mechanical Behavior of Materials, The Hague, The Netherlands, 1995.
18. S. Wu, *Polym. Eng. Sci.,* **27,** 335 (1988).
19. D. Dompas and G. Groeninckx, *Polymer,* **35,** 4743 (1994).